iomac
International Operational Modal Analysis Conference

11th International Operational Modal Analysis Conference

20 - 23 May 2025 | Rennes, France

Vibration analysis of a car door using randomly sampled stereo camera measurements with a large stereo angle

Yonggang Wang[1,2] ✉, *Thijs Willems*[1,2], *Nathan Dwek*[1,2], *Matteo Krichner*[1,2], *Frank Naets*[1,2]

✉ yonggang.wang@kuleuven.be

[1] Department of Mechanical Engineering, KU Leuven, Celestijnenlaan 300, B-3001, Heverlee, Belgium

[2] Flanders Make@KU Leuven, Flanders Make, Belgium

ABSTRACT

Vibration analysis techniques, such as modal analysis, are widely used to assess the dynamic properties of mechanical components and systems. Traditional methods rely on sensors (*e.g.,* accelerometers) to measure vibrations; however, these sensors can alter the mass and damping properties of the system and require multiple tests to obtain spatially dense information. Cameras offer an alternative for vibration analysis, providing the usual advantages of contactless measurement, such as adding no mass or damping and offering high spatial resolution. Using a stereo camera setup enables 3D displacement measurements, which require accurate point matching between the cameras and consistent point tracking across video frames. Despite the potential of camera-based measurements, limitations in frame rate present a challenge. In this study, a previously developed random sampling framework is employed to capture high-frequency vibration signals at a low equivalent frame rate. To improve out-of-plane measurement accuracy, a large stereo angle (38° in this experiment) between cameras is preferred, although this angle introduces challenges in point matching. This study presents an approach for matching dense point pairs through image registration with projective transformation, based on initial point matches. Point tracking is accomplished using the Lucas-Kanade optical flow algorithm, a simplified approach to digital image correlation. Experimental testing on a car door, at an equivalent frame rate below 130 frames per second, identified 10 vibration modes up to 139 Hz using hammer excitations (*i.e.,* approximately twice the Nyquist limit). Several excitation locations were tested, revealing that the excitation at the door corner should be avoided, as it affects wave transmission and deflection shape measurements.

Keywords: Stereo cameras, Displacement measurement, Vibration analysis, random sampling

1. INTRODUCTION

Modal Analysis assesses the dynamic behavior of vibrating objects under excitation [1], including Experimental Modal Analysis (EMA) and Operational Modal Analysis (OMA). EMA requires a known excitation (*e.g.*, impact hammer or shaker), while OMA handles unknown or uncontrolled excitation(s). OMA is preferable when excitation measurements are unavailable or operational conditions affect dynamics [2–5], whereas EMA suits laboratory settings and provides reliable damping estimates [6–8]. This work focuses on OMA due to the unavailability of the excitation signal.

In OMA, vibration signals are traditionally measured with accelerometers and strain gauges, but limited sensors and data channels restrict the spatial density of the vibration measurements. Cameras capture full-field displacements, enabling detailed modal analysis, though their lower frame rate limits high-frequency data capture [9, 10]. Reducing the Region of Interest (ROI) increases the frame rate but lowers spatial resolution and displacement sensitivity. To extend the measurable frequency range, a random sampling framework was proposed [10]. By capturing images randomly in time, high-frequency responses can be reconstructed using a nonlinear optimization model, though low-amplitude high-frequency modes may be lost due to camera noise. Accurate displacement measurement requires optimized image resolution, lighting, and camera positioning, with this study focusing on the stereo angle (*i.e.*, the angle between the optical axes of the two cameras) in 3D measurements.

To have a high accuracy of the out-of-plane displacement in the 3D measurements, a large stereo angle is preferred [11]. However, a large stereo angle complicates the stereo feature point matching and reduces measurement accuracy [12]. In the literature, feature point matching algorithms are categorized into two strategies. The first strategy, structure from motion, tracks points from Camera 1 to Camera 2 using optical flow or digital image correlation. This strategy is suitable when camera views are similar, as the adopted tracking algorithms assume small displacements. The second strategy relies on feature extraction algorithms (SIFT, SURF, ORB) [13], and the extracted feature points are matched with RANSAC or brute force [14]. Although the second strategy is able to handle large view differences, a large stereo angle decreases the number of matched points.

This study proposes an approach for matching dense point pairs using image registration with projective transformation, based on initial matches from feature extraction and matching. The paper is structured as follows: Section 2. discusses prior work on the random sampling strategy and the proposed image registration for feature point matching. Section 3. presents experimental validation through the OMA of a pseudo-free suspended car door. Finally, section 4. provides a summary and future insights.

2. METHODOLOGY: RANDOM SAMPLING AND IMAGE REGISTRATION

2.1. Randomly sampled camera measurements

The procedure for measuring 2D displacements with a single camera includes camera calibration, image acquisition, image pre-processing, feature point detection, and feature point tracking. 3D displacement measurements require a stereo setup consisting of at least two cameras, and feature point matching between the cameras and triangulation are required [15].

In the random sampling framework, the displacement measured by the cameras is randomly sampled over time. The displacement signal is then reconstructed at a high sampling frequency for OMA. In practice, the first step is to record videos of a vibrating structure while triggering the stereo cameras randomly. The time intervals between consecutive video frames are uniformly distributed within the range of Δt_{min} to $2\Delta t_{min}$, where Δt_{min} is the inverse of the highest frame rate supported by the hardware.

In the second step, displacements are measured using a tracking algorithm such as the Lucas-Kanade optical flow algorithm, with an attached pattern to enhance measurement accuracy. The third step aims to fit the measured displacements at a given location. A nonlinear optimization model, derived from the Impulse Response Functions, is formulated to recover the high-frequency displacements in [10]. When

the excitation is an impact force or a pseudo-random excitation in OMA, the structural responses can be approximated as a sum of damped sine waves. The nonlinear optimization model is presented as follows:

$$\underset{A_i,\lambda_i,\varepsilon}{\arg\min} \left\| \sum_{i=1}^{N} \Re(A_i e^{\lambda_i t_m}) - y(t_m) - \varepsilon \right\|_2^2, \tag{1}$$

Here A_i and λ_i are complex numbers. λ_i is defined by $2\pi f_i j - \sigma_i$, including eigenfrequency f_i and damping factor σ_i. N is the number of eigenfrequencies, and $\|\cdot\|_2$ denotes the Euclidean norm of a vector. The term ε represents a constant offset when the mean amplitude is nonzero. t_m represents the randomly sampled time vector. The term $y(t_m)$ denotes the randomly sampled displacement measurements at a specific location.

This optimization problem can be solved using a gradient-based algorithm, which requires an initial guess of the eigenfrequencies $f_i,\ i = 1, \ldots, N$. The initial guess is obtained from the measurements of the additional accelerometers, and conditions the accuracy of the recovered deflection shapes. The recovered displacements are subsequently used for vibration analysis.

The nonlinear optimization in eq. (1) can be time-consuming. As an alternative, a linear model can be adopted by neglecting the damping to accelerate reconstruction:

$$y(t_m) = \Re\left(\Psi s\right). \tag{2}$$

Here, Ψ consists of Fourier basis functions, with each column defined as $e^{-j2\pi f_i t_m}/\sqrt{N}$. The least-square solution for s is computed using MATLAB's *mldivide* function. For signal reconstruction, Ψ_r is formed as $e^{-j2\pi f_i t_s}/\sqrt{N}$ using the time vector t_s, where t_s represents a regularly sampled time vector at a high sampling frequency. The structural response at each measurement position is then recovered as $\Re(\Psi_r s)$ at a high sampling frequency. This linear fitting model is used as a point of comparison in section 3..

2.2. Image feature point matching

The reduced accuracy in feature point matching arises from the significant view difference between stereo cameras, *i.e.,* camera 1 and camera 2. To address this difference, it is required to analyze the transformation between the cameras' images.

When the vibrating object is a flat plate, its projection onto the camera plane follows a linear mapping. This projection adheres to a projective transformation, which is represented by a 3×3 transformation matrix T [16]. The matrix T maps a point (u, v) in the input coordinate system to a point (x, y) in the output coordinate system based on:

$$\begin{bmatrix} x' \\ y' \\ k \end{bmatrix} = T \begin{bmatrix} u \\ v \\ 1 \end{bmatrix} \tag{3}$$

where k is a scale factor, and the transformed coordinates are given by $x = x'/k$ and $y = y'/k$. Since the transformation described in eq. (3) is reversible, the flat plate, its projection on the image plane of camera 1, and its projection on the image plane of camera 2 all maintain projective transformation relationships with one another. By leveraging this projective transformation, the images captured by both cameras can be aligned. Through pre-processing, the differences between the image pair are corrected, enabling accurate dense feature point matching via point tracking.

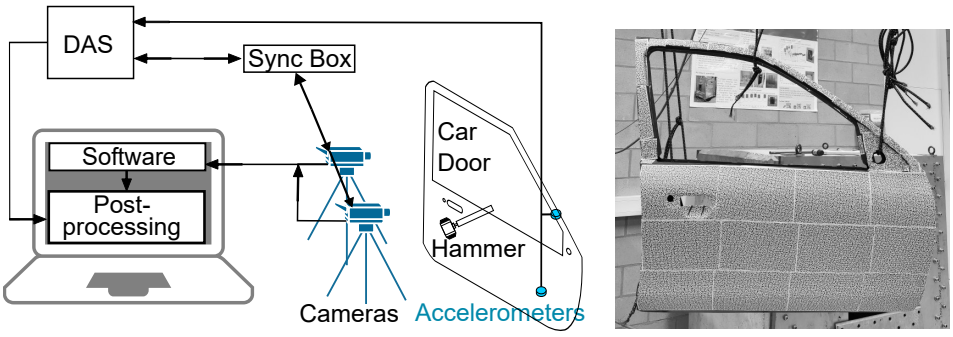

Figure 1: Experimental setup for OMA of the car door: (a) data acquisition (b) car door with speckle pattern.

The transformation matrix T between images is computed based on initially matched feature points obtained through feature point extraction and matching. In this study, SURF features are selected to establish the initial point pairs, as they have been observed to yield the highest number of feature point correspondences [13]. Using this transformation, the images are registered, reducing discrepancies between them. A tracking algorithm is then employed to track dense points from the image of camera 1 to the image of camera 2, resulting in a dense set of point pairs.

When the object is not a flat plate, the image is divided into multiple regions that are approximately planar. Feature point matching is performed separately within each region, and the resulting feature point pairs are then combined to achieve 3D displacement measurements with high spatial density.

3. OPERATIONAL MODAL ANALYSIS OF THE CAR DOOR

To validate the proposed method, a car door suspended by two bungee cords is used as the test object. The experimental setup and geometry are illustrated in fig. 1, where DAS stands for data acquisition system. Two accelerometers are utilized: one single-axis accelerometer [17] and one three-axis accelerometer [18]. Their measurements allow to accurately estimate the eigenfrequencies, which are then used for signal reconstruction in the camera-based measurements.

A partial Operational Modal Analysis (OMA) is performed on the accelerometer data, employing the polyreference Least-Square Complex Frequency domain (pLSCF) method [19]. To generate the stabilization diagram in OMA, the covariance of the acceleration spectra is computed. The accelerometer data is processed using the operational PolyMAX module in Simcenter [20], and 10 eigenfrequencies below $150\,\mathrm{Hz}$ are selected.

Stereo cameras [21, 22] are used to capture the 3D displacements of the car door induced by the hammer excitation. A random sampling strategy is adopted, with the maximum frame rate set to 130 frames per second (fps). The cameras operate at full resolution (4096×3072 pixels) with an 8-bit depth and an exposure time of $3\,\mathrm{ms}$. During stereo camera data processing, matched feature points in the stereo image pair are identified using the proposed image registration method. For comparison, the conventional point-tracking method is also implemented, utilizing the 2D digital image correlation program *Ncorr* to track a predefined grid of points [23]. Due to the significant view difference, an initial displacement estimate is required for successful tracking using *Ncorr*. In this case, the estimation is obtained by tracking a manually selected corner of the car door. The accuracy of these two methods for point matching is assessed using the re-projection error. This error is determined by projecting each world point back into both images and calculating the distance between the detected and re-projected points. The distances in the two images are then averaged to obtain the final re-projection error. The histograms of the re-projection errors are presented in fig. 2, demonstrating that the proposed image registration method

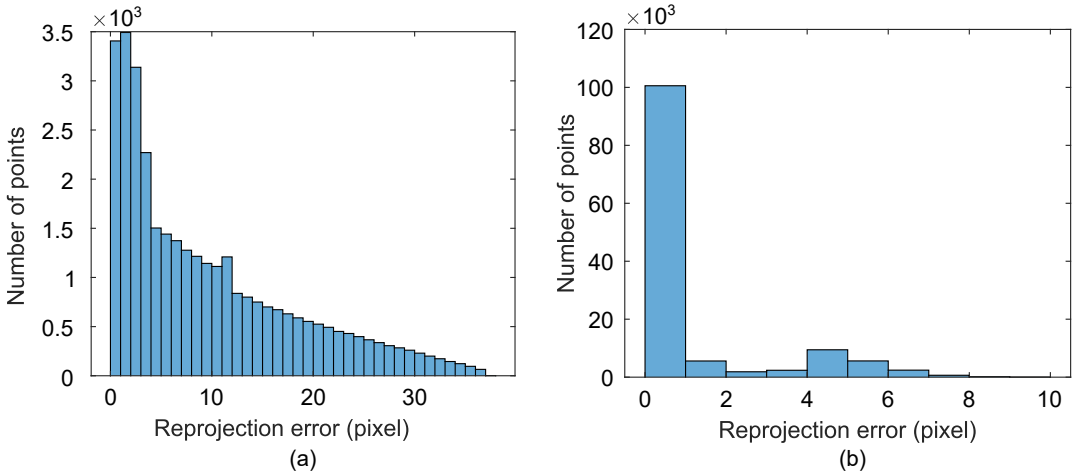

Figure 2: Point matching error histograms: (a) conventional point tracking with initial displacement given, and (b) proposed method.

yields a greater number of matched points with lower re-projection error. Despite providing *Ncorr* with a good initial guess to facilitate tracking, the image differences still lead to inaccuracies in point tracking.

Since the camera data is randomly sampled, high-frequency signals must be reconstructed. In the reconstruction process, the eigenfrequencies measured by accelerometers are set as the frequency components of the signal. The reconstruction is performed using a nonlinear optimization model (eq. (1)). After reconstruction, the spectrum of the reconstructed signal is analyzed using the polyreference Least-Square Complex Frequency domain (pLSCF) method to extract the operational deflection shapes of the car door. The results of the OMA on the reconstructed signal using the nonlinear approach are presented in fig. 3. For comparison, OMA is also conducted using the reconstructed signal obtained from the linear fitting approach, and the deflection shape at $101.0\,\mathrm{Hz}$ is presented in fig. 3. From the visualization, it is observed that the linear fitting approach produces less noisy results; however, the spatial peaks in the deflection shape are not well separated. Since damping is neglected in the linear fitting approach, the residuals from the low-frequency fitting propagate into the high-frequency deflection shapes. The nonlinear optimization approach exhibits high random noise due to numerical errors. The correlation between these deflection shapes is quantified using the auto Modal Assurance Criteria (MAC), as shown in fig. 4. The results demonstrate that the random sampling strategy effectively separates the different eigenfrequency components.

Different excitation positions were tested, and the results presented in fig. 3 correspond to the position marked by the hammer head in fig. 1. Alternatively, when the car door was struck at the corner, strong wave propagation was observed in that region, altering the measured deflection shapes. This effect could be attributed to the nonlinear behavior of the car door.

4. CONCLUSIONS

This study demonstrates the effectiveness of a random sampling approach for high-frequency vibration analysis using stereo cameras. By applying this technique, high-frequency vibration components were successfully reconstructed beyond the Nyquist limit. The method was validated through operational modal analysis on a pseudo-free suspended car door, where both linear and nonlinear fitting techniques were explored for signal reconstruction. While the linear fitting approach is computationally efficient, it introduces residual errors in the estimated deflection shapes due to the damping not being modeled.

To improve the accuracy of 3D displacement measurements, an image registration technique was implemented for improved feature point matching. This approach effectively addresses challenges posed by large stereo angles, ensuring high spatial density in displacement measurements. Additionally, the

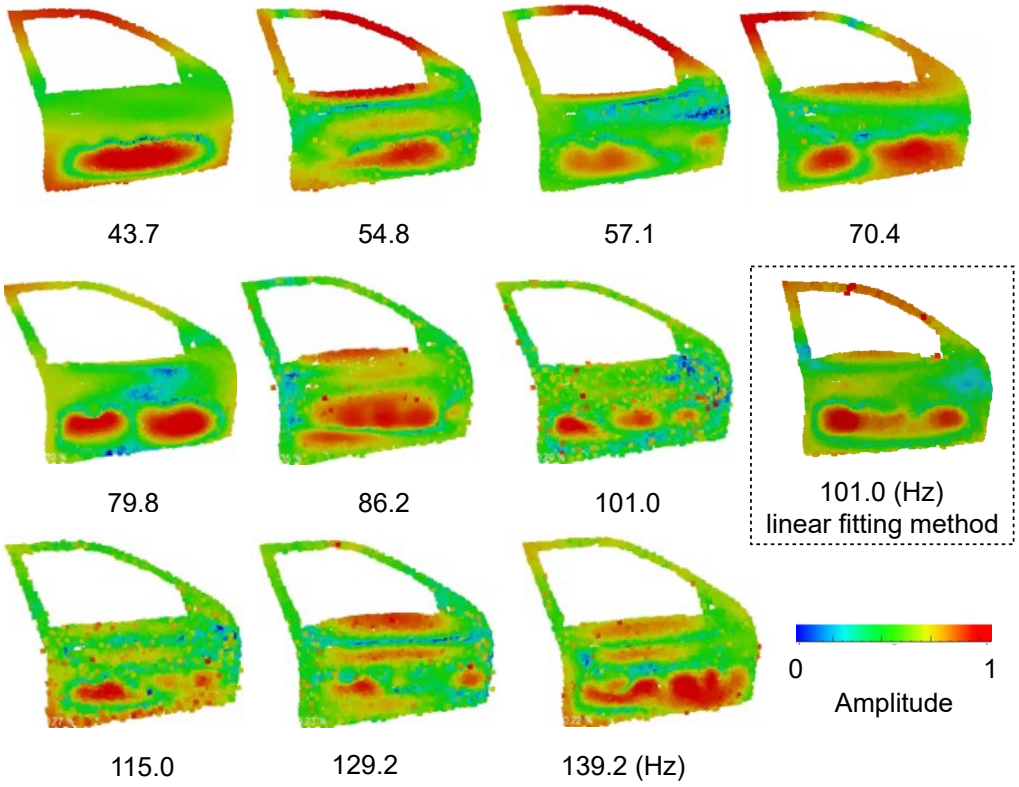

Figure 3: Operational deflection shapes obtained from randomly sampled camera data.

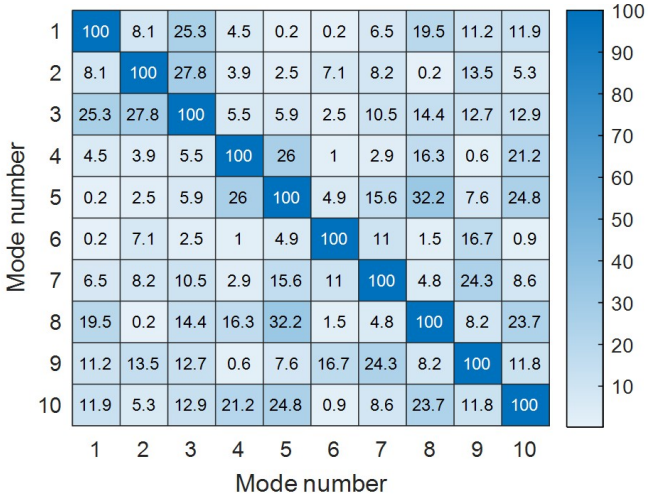

Figure 4: Auto MAC of the deflection shapes.

proposed method shows potential for large-scale motion tracking with sub-pixel accuracy, as it addresses challenges posed by significant view differences and the assumption of small displacements.

ACKNOWLEDGMENTS

This research was partially supported by Flanders Make, the strategic research centre for the manufacturing industry. The Research Foundation Flanders (FWO) is gratefully acknowledged for its support through research grant no. G095120N. Furthermore, Internal Funds KU Leuven are gratefully acknowledged for their support.

REFERENCES

[1] Edwin Reynders. System identification methods for (operational) modal analysis: Review and comparison. *Archives of Computational Methods in Engineering*, 19(1):51–124, February 2012. ISSN 1886-1784. doi: 10.1007/s11831-012-9069-x. URL `http://dx.doi.org/10.1007/s11831-012-9069-x`.

[2] Rune Brincker and Carlos Ventura. *Introduction to operational modal analysis*. John Wiley & Sons, 2015.

[3] Martin D Ulriksen, Dmitri Tcherniak, Poul H Kirkegaard, and Lars Damkilde. Operational modal analysis and wavelet transformation for damage identification in wind turbine blades. *Structural Health Monitoring: An International Journal*, 15(4):381–388, July 2016. doi: 10.1177/1475921715586623.

[4] Peyman Poozesh, Javad Baqersad, Christopher Niezrecki, Peter Avitabile, Eric Harvey, and Rahul Yarala. Large-area photogrammetry based testing of wind turbine blades. *Mechanical Systems and Signal Processing*, 86:98–115, March 2017. doi: 10.1016/j.ymssp.2016.07.021.

[5] Yongchao Yang and Satish Nagarajaiah. Output-only modal identification by compressed sensing: Non-uniform low-rate random sampling. *Mechanical Systems and Signal Processing*, 56-57:15–34, May 2015. doi: 10.1016/j.ymssp.2014.10.015.

[6] Esben Orlowitz and Anders Brandt. Comparison of experimental and operational modal analysis on a laboratory test plate. *Measurement*, 102:121–130, May 2017. doi: 10.1016/j.measurement.2017.02.001.

[7] Carmine Maria Pappalardo and Domenico Guida. System identification and experimental modal analysis of a frame structure. *Engineering Letters*, 26(1), 2018.

[8] A. Cusano, P. Capoluongo, S. Campopiano, A. Cutolo, M. Giordano, F. Felli, A. Paolozzi, and M. Caponero. Experimental modal analysis of an aircraft model wing by embedded fiber bragg grating sensors. *IEEE Sensors Journal*, 6(1):67–77, 2006. doi: 10.1109/JSEN.2005.854152.

[9] Ward Heylen, Stefan Lammens, Paul Sas, et al. *Modal analysis theory and testing*, volume 200. Katholieke Universiteit Leuven Leuven, Belgium, 1997.

[10] Yonggang Wang, Felix Simeon Egner, Thijs Willems, Matteo Kirchner, and Wim Desmet. Camera-based experimental modal analysis with impact excitation: Reaching high frequencies thanks to one accelerometer and random sampling in time. *Mechanical Systems and Signal Processing*, 170:108879, May 2022. doi: 10.1016/j.ymssp.2022.108879.

[11] Xingjian Liu, Wenyuan Chen, Harikrishnan Madhusudanan, Linghao Du, and Yu Sun. Camera orientation optimization in stereo vision systems for low measurement error. *IEEE/ASME Transactions on Mechatronics*, 26(2):1178–1182, April 2021. ISSN 1941-014X. doi: 10.1109/tmech.2020.3019305. URL `http://dx.doi.org/10.1109/TMECH.2020.3019305`.

[12] Elizabeth MC Jones, Mark A Iadicola, et al. A good practices guide for digital image correlation. *International Digital Image Correlation Society*, 10:308–312, 2018. doi: 10.32720/idics/gpg.ed1.

[13] Shaharyar Ahmed Khan Tareen and Zahra Saleem. A comparative analysis of sift, surf, kaze, akaze, orb, and brisk. In *2018 International Conference on Computing, Mathematics and Engineering Technologies (iCoMET)*, pages 1–10, 2018. doi: 10.1109/ICOMET.2018.8346440.

[14] Olof Enqvist, Fangyuan Jiang, and Fredrik Kahl. A brute-force algorithm for reconstructing a scene from two projections. In *CVPR 2011*, pages 2961–2968, 2011. doi: 10.1109/CVPR.2011.5995669.

[15] Yonggang Wang, Felix Simeon Egner, Thijs Willems, Frank Naets, and Matteo Kirchner. Using multi-sine excitation and rigid body motion compensation in randomly sampled camera-based experimental modal analysis to improve SNR. *Mechanical Systems and Signal Processing*, 204: 110763, 12 2023. doi: 10.1016/j.ymssp.2023.110763.

[16] Projective transformations. URL `https://homepages.inf.ed.ac.uk/rbf/CVonline/LOCAL_COPIES/BEARDSLEY/node3.html`. Accessed: 2025-01-31.

[17] Miniature, lightweight (0.8 gm) ceramic shear icp accelerometer, model 352a24, . URL `https://www.pcb.com/products?m=352A24`. Accessed: 2025-02-12.

[18] Accelerometer, icp, triaxial, model 356a02, . URL `https://www.pcb.com/products?m=356a02`. Accessed: 2025-02-12.

[19] Bart Peeters, Herman Van der Auweraer, Patrick Guillaume, and Jan Leuridan. The polymax frequency-domain method: a new standard for modal parameter estimation? *Shock and Vibration*, 11(3, 4):395–409, 2004.

[20] Simcenter testlab software. URL `https://plm.sw.siemens.com/en-US/simcenter/physical-testing/testlab/`. Accessed: 2023-07-27.

[21] Ximea xib-64 cb120rg-cm-x8g3. URL `https://www.ximea.com/products/pci-express-high-speed-cameras-xib/cb120rg-cm`. Accessed: 2022-05-17.

[22] Jai sp-12000m-cxp4. URL `https://www.jai.com/products/sp-12000m-cxp4`. Accessed: 2022-05-17.

[23] Ncorr v1.2: open source 2d digital image correlation matlab program. URL `https://www.ncorr.com/`. Accessed: 2025-02-05.